

**JMB**Available online at [www.sciencedirect.com](http://www.sciencedirect.com)

SCIENCE @ DIRECT®



## An Allosteric Model for Transmembrane Signaling in Bacterial Chemotaxis

**Christopher V. Rao<sup>1,2\*</sup>, Michael Frenklach<sup>2,3</sup> and Adam P. Arkin<sup>1,2,4</sup>**

<sup>1</sup>Department of Bioengineering  
University of California  
Berkeley, CA 94720, USA

<sup>2</sup>Lawrence Berkeley National  
Laboratory, Berkeley, CA 94720  
USA

<sup>3</sup>Department of Mechanical  
Engineering, University of  
California, Berkeley, CA 94720  
USA

<sup>4</sup>Howard Hughes Medical  
Institute, Berkeley, CA 94720  
USA

Bacteria are able to sense chemical gradients over a wide range of concentrations. However, calculations based on the known number of receptors do not predict such a range unless receptors interact with one another in a cooperative manner. A number of recent experiments support the notion that this remarkable sensitivity in chemotaxis is mediated by localized interactions or crosstalk between neighboring receptors. A number of simple, elegant models have proposed mechanisms for signal integration within receptor clusters. What is lacking is a model, based on known molecular mechanisms and our accumulated knowledge of chemotaxis, that integrates data from multiple, heterogeneous sources. To address this question, we propose an allosteric mechanism for transmembrane signaling in bacterial chemotaxis based on the “trimer of dimers” model, where three receptor dimers form a stable complex with CheW and CheA. The mechanism is used to integrate a diverse set of experimental data in a consistent framework. The main predictions are: (1) trimers of receptor dimers form the building blocks for the signaling complexes; (2) receptor methylation increases the stability of the active state and retards the inhibition arising from ligand-bound receptors within the signaling complex; (3) trimer of dimer receptor complexes aggregate into clusters through their mutual interactions with CheA and CheW; (4) cooperativity arises from neighboring interaction within these clusters; and (5) cluster size is determined by the concentration of receptors, CheA, and CheW. The model is able to explain a number of seemingly contradictory experiments in a consistent manner and, in the process, explain how bacteria are able to sense chemical gradients over a wide range of concentrations by demonstrating how signals are integrated within the signaling complex.

© 2004 Elsevier Ltd. All rights reserved.

**Keywords:** chemotaxis; allostery; receptor clustering; signal transduction; Monte Carlo

\*Corresponding author

### Introduction

Chemotaxis is the process by which cells sense changes in their chemical environment and move to more favorable conditions.<sup>1</sup> In enteric bacteria such as *Escherichia coli*, cells bias their motion in chemical gradients by transitioning between straight runs and re-orientating tumbles through the rotation of the flagella that dot their surface. The primary signal transduction module for the chemotaxis pathway involves a stable, ternary signaling complex comprising transmembrane receptors, CheW

adaptor proteins, and CheA histidine kinases,<sup>2</sup> where both the receptors and the CheA kinase form homodimers. *E. coli* cells modulate the frequency of runs and tumbles by regulating the rate of CheA autophosphorylation.<sup>3</sup> The phosphoryl-group on CheA is transferred to a soluble, cytoplasmic response regulator (CheY) that interacts with the flagellar motor and increases the likelihood of re-orienting tumbles.<sup>4</sup> A dedicated phosphatase CheZ enhances the rate of CheY dephosphorylation. *E. coli* cells respond only to temporal changes in the concentration of chemoeffector and perfectly adapt their sensory response in reference to the background stimuli. In particular, their stimulated response always returns to pre-stimulus values despite the sustained presence of attractants or repellents. Methylation of the receptors increases

Abbreviation used: TD, trimer of receptor dimers.  
E-mail address of the corresponding author:  
[c\\_rao@lbl.gov](mailto:c_rao@lbl.gov)

the rate of CheA autophosphorylation and decreases the sensitivity of receptors to attractants. The antagonizing action of the receptor methyltransferase CheR and methyl-esterase CheB adapts the sensory response by adding and removing methyl groups on the chemoreceptors.<sup>5,6</sup>

While the basic mechanism for adaptation in enteric bacteria has been elucidated and numerous mathematical models have been proposed,<sup>7–12</sup> one unresolved question is how bacteria are able to sense chemical gradients over a wide range of concentrations.<sup>13,47</sup> The signaling gain, measured as the fractional change in signaling response per fractional change in ligand concentration, is roughly constant over a range of concentrations spanning five orders of magnitude *in vivo*.<sup>14,15</sup> However, *in vitro* data suggest only a limited range.<sup>5,16</sup> The models based on these *in vitro* data predict that the gain is constant over a range of concentrations spanning one to two orders of magnitude. This difference between the models and experiments, both *in vitro* and *in vivo*, demonstrates that the current understanding for chemotaxis is incomplete and additional mechanisms are necessary to explain the signaling gain.

As the ternary signaling complexes localize at the poles of the cell,<sup>17–19</sup> the most popular explanation for sensitivity is that the receptor complexes aggregate to form higher-order structures. One model, advocated by Bray and colleagues, proposes that the chemoreceptors form a cooperative lattice.<sup>20–23</sup> In their model, a single ligand-bound receptor interacts with neighboring receptors, propagating the inhibiting signal to adjacent receptors in the lattice. While this model is appealing, as it can explain how subtle changes in the concentration of ligand elicit large responses, there is little evidence to suggest the existence of a globally cooperative lattice beyond polar localization. Furthermore, *in vivo* and *in vitro* experiments paint a mixed picture regarding cooperativity, where some experiments measure little and others measure a lot.<sup>24</sup>

On the other hand, there is substantial experimental evidence to suggest localized interactions among the individual receptor dimers. The first evidence is that the cytoplasmic domains of the serine receptor crystallize to form trimers of receptor dimers.<sup>25</sup> Using this crystal structure along with the atomic structures for CheW and CheA, Shimizu and colleagues proposed a structural model for the ternary signaling complex where three receptor dimers form a complex with three CheW monomers and three CheA dimers.<sup>23</sup> The second line of evidence is that mixed receptors interact with one another. There are five different kinds of chemoreceptors in *E. coli*, each specialized to particular chemical signals. Using genetic and crosslinking experiments, Parkinson and colleagues demonstrated that the serine (Tsr) and aspartate (Tar) receptors interact with one another in complexes consistent with the “trimer of dimers” model.<sup>26,27</sup> In  $\Delta cheBR$  cells, the sensitivity to aspartate is amplified when Tsr is deleted.<sup>15,28</sup>

Using the data reported by Sourjik & Berg,<sup>15</sup> Mello & Tu<sup>29</sup> argued that the interactions between different kinds of receptors enable cells to sense gradients over a wide range of concentrations. Further evidence is provided from the analysis of the low-abundance receptor Trg; multivalent ligands directed towards the Trg receptor amplify the response of the Tsr receptor to serine.<sup>30</sup>

In a recent series of experiments,<sup>31</sup> Sourjik & Berg measured significant cooperativity *in vivo*. Remarkably, they were able to modulate the cooperativity by independently varying the expression of receptors, CheW, and CheA. Their results demonstrate that receptors potentially interact with each other in large complexes, though the structure of these complexes is still unknown. Their results also potentially explain the discrepancy between previous cooperativity measurements, if we attribute the differences to disparities in expression. Finally, Sourjik & Berg were able to establish that different kinds of receptors interact with one another in a dose-dependent fashion, clearly establishing the existence of cooperative structures.

A number of simple, elegant models have proposed mechanisms for signal integration within receptor clusters.<sup>20,29</sup> What is lacking is a model, based on known molecular mechanisms and our accumulated knowledge of chemotaxis, that integrates data from multiple, heterogeneous sources. To address this question, we propose a two-state allosteric mechanism based on the trimer of dimers structural model to explain how bacteria sense chemical gradients over a wide range of concentrations. We explore this allosteric mechanism using numerical simulations and demonstrate that the associated model is able to explain a number of *in vitro* and *in vivo* experiments. The main predictions are: (1) trimers of receptor dimers form the building blocks for the signaling complexes; (2) receptor methylation increases the stability of the active state and retards the inhibition arising from ligand-bound receptors within the signaling complex; (3) trimer of dimer receptor complexes aggregate into clusters through their mutual interactions with CheA and CheW; (4) cooperativity arises from neighboring interaction within these clusters; and (5) cluster size is determined by the concentration of receptors, CheA, and CheW. Numerous other models have advanced alternative hypotheses,<sup>7,20,21,29,32,33</sup> and the model proposed here does not necessarily argue against any of these mechanisms. Rather, our goal was to explore a molecular mechanism involving a minimal number of assumptions that is consistent with what is known about chemotaxis, able to explain both the *in vitro* and *in vivo* data, and does not introduce additional mechanisms such as long-range signaling<sup>20</sup> or mechanisms involving dynamics clustering or feedback.<sup>7,22,32</sup>

## Theory: Assumptions and Models

We propose a two-state allosteric model for

receptor signaling akin to the Monod, Wyman, and Changeux (MWC) allosteric model.<sup>34</sup> The allosteric mechanism invokes the molecular model proposed by Shimizu and colleagues,<sup>23</sup> where three receptor dimers form a stable complex with three CheW proteins and three CheA dimers. Using the metaphors of allostery, the model assumes that the entire complex exists in either a tense or relaxed form, where the tense form corresponds with the active state and the relaxed form corresponds with the inactive state. Implicit in the allosteric model is the assumption that the associated CheA kinases within the complex act in unison. The rate of CheA autophosphorylation is proportional to the probability that the receptor complex exists in an active state. The model assumes that receptor methylation increases the stability of the active (or tense) state, whereas ligand destabilizes the active state and increases the probability that the complex will adopt an inactive (or relaxed) state. Methylation increases the stability of the receptor complex by retarding the destabilizing effect of ligand. A key assumption is that the sensitivity to ligand is primarily determined by the cooperative interactions of the receptors within the complex.

The model is supported by the following experiments. Numerous lines of experimental evidence indicate that transmembrane signaling is accomplished by a subtle conformational shift between the helices of a receptor dimer<sup>35</sup> and the receptor dimers within the signaling complex.<sup>36</sup> Using molecular models for the serine receptor and crystallography data, it was shown that inactive receptors are more dynamic than active receptors in terms of the average temperature factor.<sup>22</sup> In the proposed mechanism, the dynamic (inactive) state corresponds with the relaxed state. The conformational shift drives the complex towards the relaxed state by weakening the interactions within the complex. *In vitro* studies with purified complexes involving identical receptors demonstrate that methylation does not significantly change the sensitivity to ligand.<sup>5,28,37</sup> Instead, receptor methylation only increases the activity of the CheA kinase.<sup>38</sup> With *in vivo* studies involving multiple kinds of receptors, methylation changes the sensitivity by several orders of magnitude.<sup>15,28</sup> These results suggest that the sensitivity is modulated through the interactions among different kinds of receptors rather than by changing the affinity for ligand.

Sourjik & Berg also used an allosteric model based on the MWC formulation to analyze their data.<sup>31</sup> However, they only considered a generic MWC model and did not investigate how different kinds of receptors within the complex alter the model. They also did not attempt to adapt their model to the particulars of signaling in bacterial chemotaxis.

To analyze the data, we first considered a model where three receptor dimers associate with CheW and CheA to form stable, independent signaling complexes (Figure 1). The trimer of dimers (TD)

model assumes that the signaling complex adopts either an active (A) or an inactive (I) conformation. Each receptor dimer within the signaling complex is either bound with ligand (1) or free (0). As individual receptor dimers exhibit half-site saturation, the model assumes that each dimer subunit binds only one ligand.<sup>39</sup> For example, the notation A010 designates an active receptor complex with the first and third subunits free and the second bound with ligand. Thus, the model has a total of eight state variables (Figure 1). The model includes four possible transitions among the states. The first is the transition from an inactive conformation (I) to an active conformation (A) and the second is the reverse transition from an active conformation (A) to an inactive complex (I). As these transitions are isomerization reactions, they were modeled as first-order reactions. For example, the probability of a transition from an inactive to an active conformation is proportional to the probability that the complex adopts an inactive conformation. The third transition occurs when ligand binds the receptor, and the fourth transition occurs when the receptor releases the ligand. We assume that there is excess ligand and modeled the ligand binding reactions also as first-order processes. If we invoke detailed balancing, then there are a total of 11 free parameters in the model that characterize the steady-state behavior. If we include dynamics, then we double the number of free parameters as we need to account for both the forward and reverse rates rather than just their ratios at steady-state. Consequently, we focused on the steady-state behavior as there are no dynamic data to test the model against nor do dynamics significantly change the predictions (results not shown).

For each ligation state in the model, we can characterize the equilibrium constant between active and inactive complexes in terms of free energy:

$$K(A_{xyz} \rightleftharpoons I_{xyz}) = \exp(-\Delta G_{xyz}^m / RT) \quad (1)$$

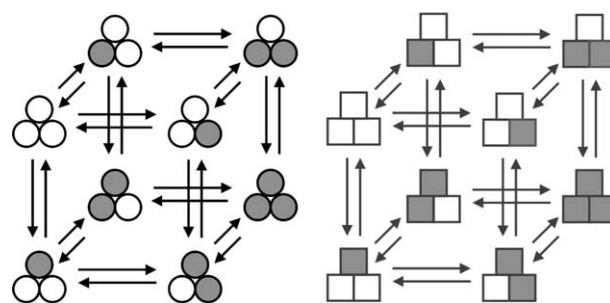


**Figure 1.** The trimer of receptor dimers (TD) allosteric model. The TD model assumes that three receptor dimers associate with CheW and CheA to form a stable complex. The model assumes that the complex exists either in an active (circles) or inactive conformation (squares). Each dimer subunit can bind one ligand (shaded circle or square). The arrows denote the transitions associated with ligand binding. The transitions between active and inactive conformations are omitted from the Figure for aesthetics.

where the subscript  $xyz$  denotes an arbitrary ligation state and the superscript  $m$  is the average number of residues methylated (the effect of differential methylation is ignored for simplicity). In terms of the physical picture, the free energy characterizes the stability of the active (or tense) state for each ligation and methylation state. Receptor methylation increases the change in free energy (e.g.  $\Delta G_{xyz}^i \leq \Delta G_{xyz}^{i+1}$ ). As the number of ligand-bound subunits increases, the free energy decreases. For example:

$$\Delta G_{000}^m \geq \Delta G_{100}^m \geq \Delta G_{110}^m \geq \Delta G_{111}^m \quad (2)$$

For complexes with the same type of receptor, the model assumes that the subunits are identical:  $\Delta G_{100}^m = \Delta G_{010}^m = \Delta G_{001}^m$  and  $\Delta G_{110}^m = \Delta G_{101}^m = \Delta G_{011}^m$ , and thus reduces the number of free parameters to five. For notational convenience, we make the definitions:  $\Delta G_0^m \triangleq \Delta G_{000}^m$ ,  $\Delta G_1^m \triangleq \Delta G_{100}^m$ ,  $\Delta G_2^m \triangleq \Delta G_{110}^m$ , and  $\Delta G_3^m \triangleq \Delta G_{111}^m$ . In addition to the change in free energy, the model distinguishes between the subunits in terms of ligand binding. The binding coefficients, for example:

$$K(A_{000} \rightleftharpoons A_{100}) \quad (3)$$

and:

$$K(A_{000} \rightleftharpoons A_{010}) \quad (4)$$

are not necessarily equal. They are equal only when the receptors are identical (e.g. Tar only) and different when the receptors are not (e.g. Tar and Tsr).

When the receptors are identical, the model assumes that methylation does not change the affinity for ligand. However, we needed to relax this assumption somewhat when applying the model to experiments involving mixed complexes of receptors. We did this by introducing a parameter  $c$  less than or equal to 1 such that:

$$\begin{aligned} cK(A_{0yz} \rightleftharpoons A_{1yz}) &= K(A_{x0z} \rightleftharpoons A_{x1z}) \\ &= K(A_{xy0} \rightleftharpoons A_{xy1}) \end{aligned} \quad (5)$$

or:

$$\begin{aligned} cK(A_{0yz} \rightleftharpoons A_{1yz}) &= cK(A_{x0z} \rightleftharpoons A_{x1z}) \\ &= K(A_{xy0} \rightleftharpoons A_{xy1}) \end{aligned} \quad (6)$$

The parameter  $c$  measures the change in ligand affinity when the receptor complexes are mixed. It suffices to consider only the high-affinity receptor for a particular ligand in a mixed complex. If the parameter  $c$  is less than 1, then the ligand affinity is decreased in mixed receptor complexes. As with the conformational changes, we parameterize the parameter  $c$  in terms of free energy:

$$c = \exp(-\Delta G_c^m / RT) \quad (7)$$

By introducing the parameter  $c$ , we are effectively assuming that receptor methylation changes the affinity for ligand.

The TD model is able to explain a number of

experiments. However, in those experiments where the measured cooperativity is greater than 3, the TD model no longer works. To include these experiments, we needed to assume that the receptors assemble into large clusters. That said, we did not wish to abandon the TD model as there is substantial evidence in favor of it. To reconcile these apparent differences, we invoked a mathematical model based on the structural model proposed by Shimizu and colleagues. In the Shimizu model,<sup>23</sup> TD receptor complexes cluster together through their shared interactions with CheW and CheA. We extended their model and assumed that each CheA dimer is able to interact with three, rather than two, TD receptor complexes with CheW as the glue in between (Figure 2(a)). This extension was necessary for the model to attain Hill coefficients greater than 6. A key element of this model is that the TD receptor complex is the smallest functional unit of receptors in a signaling complex.

There are two components to the clustered TD model. The first component dealt with the size and structure of the cluster (Figure 2(b)). To model cluster formation, we extended the lattice model proposed by Bray and colleagues<sup>40</sup> and simulated cluster formation using the Metropolis algorithm. In this model, TD receptor complexes randomly diffuse and rotate on a hexagonal lattice. CheW can

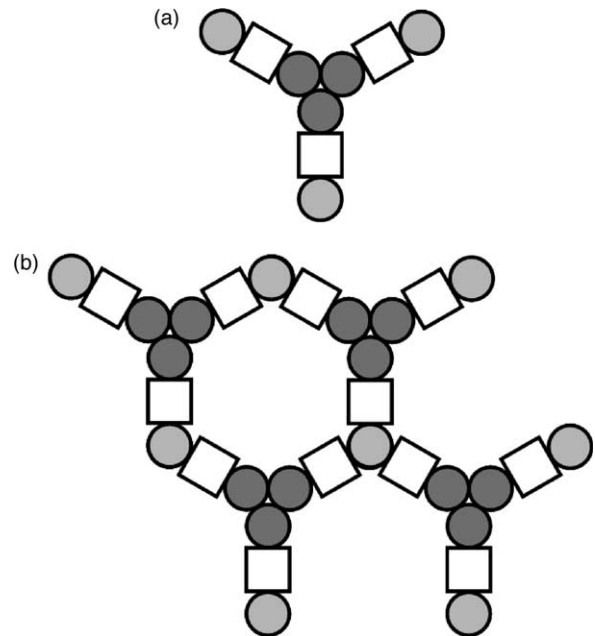


**Figure 2.** (a) Isolated trimer of dimers signaling complex. The dark gray circles denote receptor dimers, the white squares denote CheW, and the light gray circles denote CheA dimers. (b) Clustered trimer of dimers signaling complex. The dark gray circles denote receptor dimers, the white squares denote CheW, and the light gray circles denote CheA dimers. Note that some CheA dimers interact with multiple receptor TD complexes depending on the structure of the cluster. Cooperativity is assumed to increase with the number of interacting TD receptor complexes.

bind to the TD receptor complexes with interaction energy  $\Delta G_{RW}$  and CheA dimers can bind to CheW with interaction energy  $\Delta G_{AW}$ . Clusters form when multiple TD receptor complexes bind to the same CheA dimer through their shared interactions with CheW. We were interested particularly in the average number of TD receptor complexes bound to a given CheA dimer, as it provides a measure of cooperativity.

The second component of the model is the allosteric mechanism governing signal transduction in the cluster. We assumed that the state of the CheA kinase, being either active or inactive, is determined by the ligation and methylation states of the TD receptor complexes coupled to it. If a single TD complex is clustered to a given CheA dimer, then the clustered TD model is identical with the allosteric mechanism discussed previously for isolated TD receptor complexes. If two or three TD complexes are clustered to a given CheA dimer, then the model extends the allosteric mechanism by increasing the number of receptor subunits from three to six or nine (depending on the cluster configuration) with appropriate corrections for the transitions among the different states. To limit the explosion in the number of free parameters, we made a few simplifying assumptions discussed in Results. As a result of this clustering formulation,

signaling is localized and does not propagate through the entire cluster as with the spin-glass models proposed by Bray and colleagues.<sup>20,21</sup> Long-range signaling is a legitimate possibility and we considered it, but did not find it necessary to integrate the data.

The clustered model is supported by a number of experiments, in particular the experimental work by Studdert & Parkinson<sup>27</sup> and Sourjik & Berg.<sup>31</sup> Using a directed crosslinking approach based on the structural model for the receptors,<sup>25</sup> Studdert & Parkinson argued that trimers of receptor dimers form the basic building blocks for the signaling complexes, as their structural integrity does not depend on CheW, CheA, methylation, or the ligation state. The connections with the Sourjik & Berg experiments are discussed in Results.

## Results

### Parametric sensitivity of homo-TD model

If we fix the ligand affinity, then four parameters characterize the TD model when the subunits are identical, which we designate the homo-TD model. To determine the parametric behavior of the homo-TD model, we plotted the fraction of active

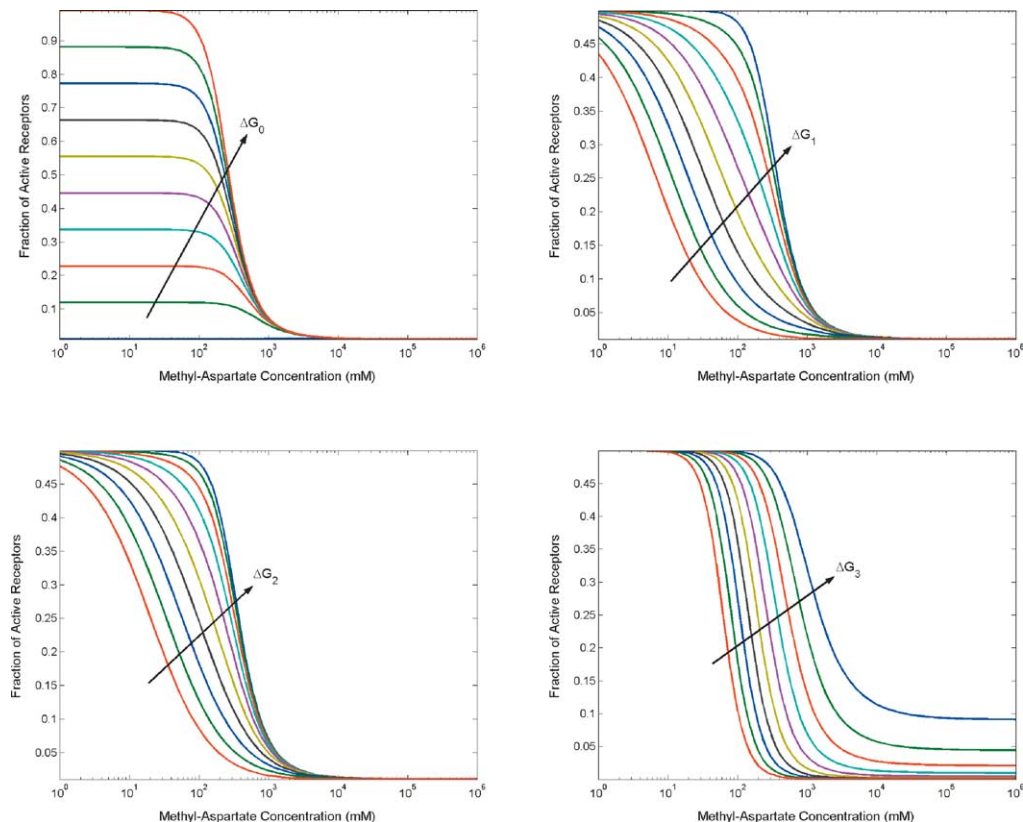


**Figure 3.** Parametric sensitivity of homo-TD model. The nominal parameters are:  $K(A_{000} \rightleftharpoons A_{100}) = 100 \mu\text{M}$ ,  $\Delta G_0 = 0 \text{ kcal/mol}$ ,  $\Delta G_1 = 0 \text{ kcal/mol}$ ,  $\Delta G_2 = \max(\Delta G_1, 0 \text{ kcal/mol})$ ,  $\Delta G_3 = -2.7 \text{ kcal/mol}$ , and  $\Delta G_c = 0 \text{ kcal/mol}$ . The remaining parameters were determined by the thermodynamic linkage conditions. The ligand-response curves were generated by varying one parameter with respect to the nominal parameters. The arrows indicate how the model changes when a specific parameter is increased.

complexes as a function of ligand concentration for different values of the four parameters (Figure 3). The free energy for the unbound receptor complex  $\Delta G_0$  increases the basal activity of the complex, as it increases the probability that the unbound complex adopts an active conformation. The free energy  $\Delta G_0$ , however, does not change the apparent  $K_m$  (defined as the half-maximal activity  $[L]_{0.5}$ ) or the cooperativity between subunits, because it only characterizes the behavior of the unbound complex. On the other hand, the free energy of the complex with one ligand-bound subunit  $\Delta G_1$  or two ligand-bound subunits  $\Delta G_2$  simultaneously increases the apparent  $K_m$  and the cooperativity, though it does not change the basal activity. Note that the affinity for ligand is not the same as the apparent  $K_m$  in the model, because the affinity is fixed separately from the free energies. As the free energies  $\Delta G_1$  and  $\Delta G_2$  increase, one or two ligand-bound subunits do not deactivate the complex; only when two or more subunits are bound with ligand is the complex deactivated. The cooperativity increases with  $\Delta G_1$  and  $\Delta G_2$ , because multiple ligand-bound subunits are necessary to deactivate the complex, hence the increase in the apparent  $K_m$  and cooperativity. The free energy of the complex when all three subunits are ligand-bound,  $\Delta G_3$ , increases the apparent  $K_m$  and the activity under saturating ligand concentrations. The increase in the apparent  $K_m$  is due to detailed balancing; increasing the free energy  $\Delta G_3$  decreases the affinity for ligand in the inactive (relaxed) state.

### Analysis of the aspartate receptor

We first compared the TD model to the data published by Bornhorst & Falke.<sup>16,37</sup> Other studies have also experimentally investigated the aspartate receptor and reported similar findings,<sup>5,28</sup> though the Bornhorst & Falke study appears to be the most comprehensive. In their *in vitro* experiments, they measured the effect of methyl-aspartate on CheA kinase activity using modified receptors with amino acid substitutions that mimic different methylation states. There are at least three major trends in their data. The first is that the kinase activity increases with the number of modifications (akin to the number of residues methylated), the second is that the apparent  $K_m$  also increases with the number of modifications, and the third is that there is limited cooperativity that changes only moderately with the modification state. All three trends correlate nicely with our previous analysis of the homo-TD model.

The TD model fits their data well (Figure 4(a)), where the estimated parameters (fitted by hand) are plotted in Figure 4(b). We see a clear trend in the parameters as a result of receptor methylation. The free energies  $\Delta G_0$ ,  $\Delta G_1$ ,  $\Delta G_2$ , and  $\Delta G_3$  all increase as the average number of modifications increases. This trend is expected, as methylation increases both the kinase activity and apparent  $K_m$ . Furthermore, changes in free energy ( $\Delta G_0 - \Delta G_1$ ) and ( $\Delta G_1 - \Delta G_2$ ) decrease as the average number of modifications

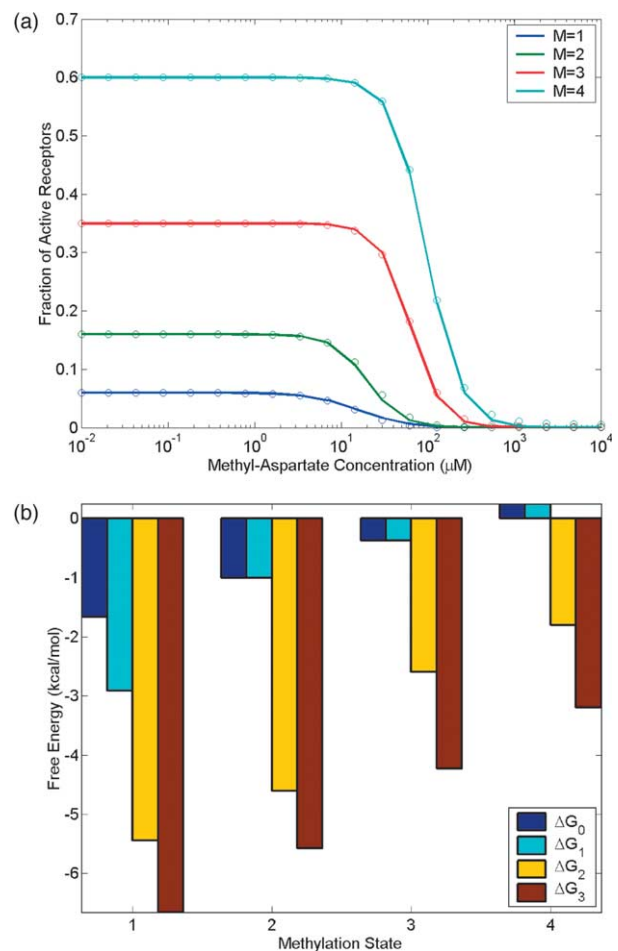


**Figure 4.** (a) Homo-TD model applied to the aspartate receptor data. The circle markers denote the model and the continuous lines denote the data for the aspartate receptor reported by Bornhorst & Falke.<sup>37</sup> We averaged their data and presented their data as the solution of the equation  $A_0 K^n / (K^n + L^n)$ , where for  $m=1$ ,  $A_0=0.06$ ,  $K=16 \mu\text{M}$ , and  $n=1.6$ ; for  $m=2$ ,  $A_0=0.16$ ,  $K=20 \mu\text{M}$ , and  $n=2.2$ ; for  $m=3$ ,  $A_0=0.35$ ,  $K=63 \mu\text{M}$ , and  $n=2.4$ ; and for  $m=4$ ,  $A_0=0.6$ ,  $K=97 \mu\text{M}$ , and  $n=2.2$ . (b) Parameters for homo-TD model. For all methylation states, the affinity for ligand is  $K(A_{000} \rightleftharpoons A_{100}) = 1 \text{ mM}$ .

increases. This trend explains how methylation increases the apparent  $K_m$ . When only a few methylation sites are modified, one or two ligand-bound subunits can destabilize the complex. As the number of modified sites increases, two or three ligand-bound subunits are needed to destabilize the complex. These results suggest, at least under the conditions measured by Bornhorst and Falke, that the signaling complex involves at least three receptor dimer subunits. Obviously, larger complexes are possible, though there are no features in the Bornhorst & Falke data to suggest more complex models.

### Analysis of the serine receptor

We next compared the model to the data

published by Li & Weis.<sup>41</sup> The Li and Weis experiments are similar to the Bornhorst & Falke experiments, except that they investigated the serine receptor instead of the aspartate receptor. However, their results are significantly different. Unlike the measurements made for the aspartate receptor,<sup>5,16,28</sup> Li & Weis found that receptor modifications strongly influence the apparent  $K_m$  (a factor of 4600, 0.2  $\mu\text{M}$  to 1 mM *versus* a factor of 6, 16  $\mu\text{M}$  to 97  $\mu\text{M}$ ). They also measured significant cooperativity, with a Hill coefficient of 5.3 for the fully modified receptor. As the Hill coefficient is so high, we were unable to fit the TD model to their data unless we assumed that the signaling complexes are clustered such that each CheA dimer was bound to at least two TD receptor complexes.

To fit the Li & Weis data to the model, we assumed that each CheA dimer was bound to two TD receptor complexes. To limit the number of parameters, we also assumed that each receptor dimer subunit within the hexamer is identical. In addition, Li & Weis measured residual kinase activity when the receptors are saturated with ligand. The clustered TD model was unable to capture this residual activity, because we had to assume that the saturated complexes were completely inactive in order to fit the measured range of apparent  $K_m$  values. If we ignore the residual activity, then the clustered TD model fits the data trends well (Figure 5(a)). The parameters are plotted in Figure 5(b), where we again see a clear trend in the parameters. For a single modification site (e.g. one residue methylated), CheA is deactivated by only one ligand-bound subunit in the cluster, whereas the fully modified receptor requires that all six subunits are bound with ligand. The large change in free energy is needed to account for the broad range of apparent  $K_m$  values. Also, for the same reasons, the change in free energy under saturating ligand conditions does not increase as the number of modification sites increases.

Clearly, the serine data suggest a different model than the aspartate receptor. In a second study,<sup>38</sup> Levit & Stock present data for the serine receptor where receptor methylation has less effect on the apparent  $K_m$  (a factor of 23, 10  $\mu\text{M}$  for unmodified receptors to 230  $\mu\text{M}$  for fully modified receptors, *versus* a factor of 4600 for the Li & Weis data). Their data also indicate that there is limited cooperativity ( $\sim 1.7$ ). We did not attempt to fit the model to the Levit & Stock data, as their results are normalized, though the trends are similar to the aspartate receptor (clearly the unclustered TD model can fit these measurements). In a third study, Sourjik & Berg<sup>31</sup> measured significant cooperativity *in vivo* ( $n=9$ ) for  $\Delta cheBR$  cells expressing only Tsr receptors, which is consistent with the Li & Weis experiments. However, they did not measure how methylation changes the effective  $K_m$ , so we did not fit their data directly. It is not definitively clear why these experimental results are significantly different, but the model predicts that the differences are

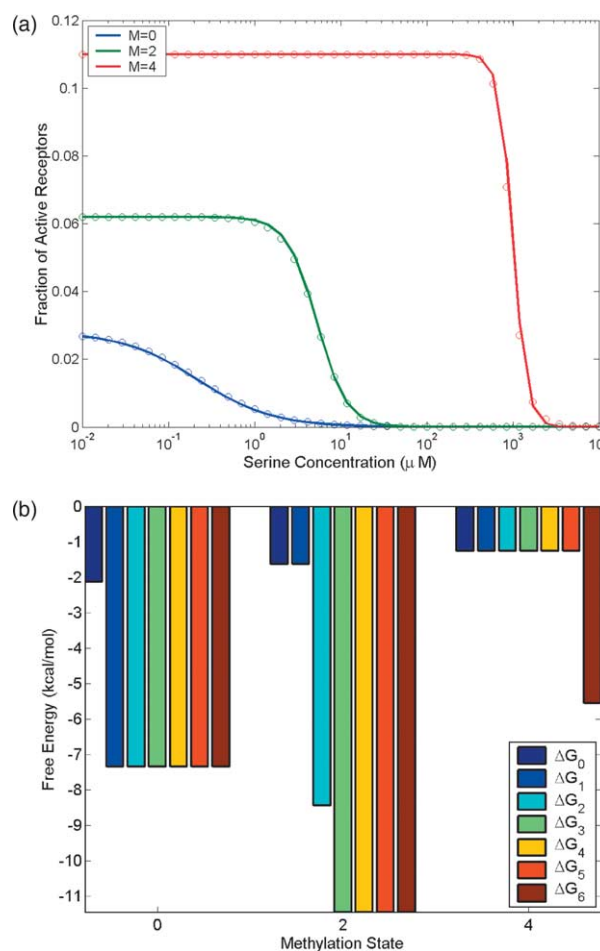


**Figure 5.** (a) Clustered TD model applied to the serine receptor data. In this model formulation, each CheA dimer associates with two TD receptor complexes. The circle markers denote the model and the continuous lines denote the serine receptor data reported by Li & Weis.<sup>41</sup> Their data are presented as the solution of the equation  $A_0 K^n / (K^n + L^n)$ , where for  $m=0$ ,  $A_0=0.028$ ,  $K=0.2 \mu\text{M}$ , and  $n=1$ ; for  $m=2$ ,  $A_0=0.062$ ,  $K=5.2 \mu\text{M}$ , and  $n=2.5$ ; and for  $m=4$ ,  $A_0=0.11$ ,  $K=1 \text{ mM}$ , and  $n=5.3$ . (b) Parameters for the clustered TD model. The parameter  $\Delta G_n$  denotes the free energy for the active state when a total of  $n$  subunits within the cluster are bound with ligand. For all methylation states, the affinity for ligand for the active state is 128  $\mu\text{M}$ .

due to the amounts of protein expressed. We elaborate in the subsection Clustering.

### Mixed TD model: aspartate and serine receptors

We next compared the TD model to the data published by Sourjik & Berg.<sup>15</sup> Unlike the previous experiments, they were able to measure the effect of methyl-aspartate on CheA kinase activity with modified receptors *in vivo*. They performed their experiments with cells expressing both aspartate (tar) and serine (tsr) receptors. Unlike the *in vitro* experiments involving solely the aspartate receptor, Sourjik and Berg measured a large change in the

apparent  $K_m$  (a factor of 3000, 2.6  $\mu\text{M}$  to 75 mM) with respect to changes in receptor methylation. They also measured two apparent  $K_m$  values in  $\Delta\text{cheBR}$  cells, where the first is due to the aspartate receptor binding methyl-aspartate at low concentrations and the second is due to the serine receptor binding methyl-aspartate at high concentrations. Mello & Tu<sup>29</sup> used these data to propose a model that predicts that the large changes in sensitivity are due to interactions between the aspartate and serine receptor. The model described next is consistent with their hypothesis and builds on their results by providing a molecular mechanism for signaling.

To analyze the Sourjik & Berg data, we needed to formulate the TD model with non-identical subunits, which we refer to here as the mixed-TD model. Because three is an odd number, we considered a mixed-TD model with two Tar receptors and one Tsr receptor and another with one Tar receptor and two Tsr receptors. Both configurations fit the Sourjik & Berg data well (Figure 6(a)). Unlike the homo-TD model, the mixed-TD model assumes that:

$$K(A_{000} \rightleftharpoons A_{100}) \neq K(A_{000} \rightleftharpoons A_{001}) \quad (8)$$

and  $\Delta G_c \neq 0$ . The estimated parameters are plotted in Figure 6(b). Again, we see a clear trend in the free energies as the number of modification sites on the aspartate receptor increases for both configurations (the serine receptors are fixed in their experiments with two sites amidated). In agreement with Mello & Tu, the model predicts that unstimulated wild-type receptor complexes are minimally methylated, corresponding to at most one residue methylated on either the Tar or Tsr receptor. Likewise, the  $\Delta\text{cheB}$  mutant data match the predictions when all of the residues on both receptors are modified and the  $\Delta\text{cheR}$  mutant data match the prediction when the receptors are unmethylated. These predictions were subsequently verified in a second study by Sourjik & Berg.<sup>31</sup>

Similar experimental trends were reported by Duntzen & Koshland,<sup>28</sup> where they showed that the range of apparent  $K_m$  values for aspartate receptor modifications in  $\Delta\text{cheBR}$  cells in response to D-aspartate increased from a range of 5–90  $\mu\text{M}$  in the absence of the serine receptor to a range of 15–3000  $\mu\text{M}$  in the presence of the serine receptor. We did not attempt to fit the model to their data as they only reported the  $K_m$ . They also reported only a

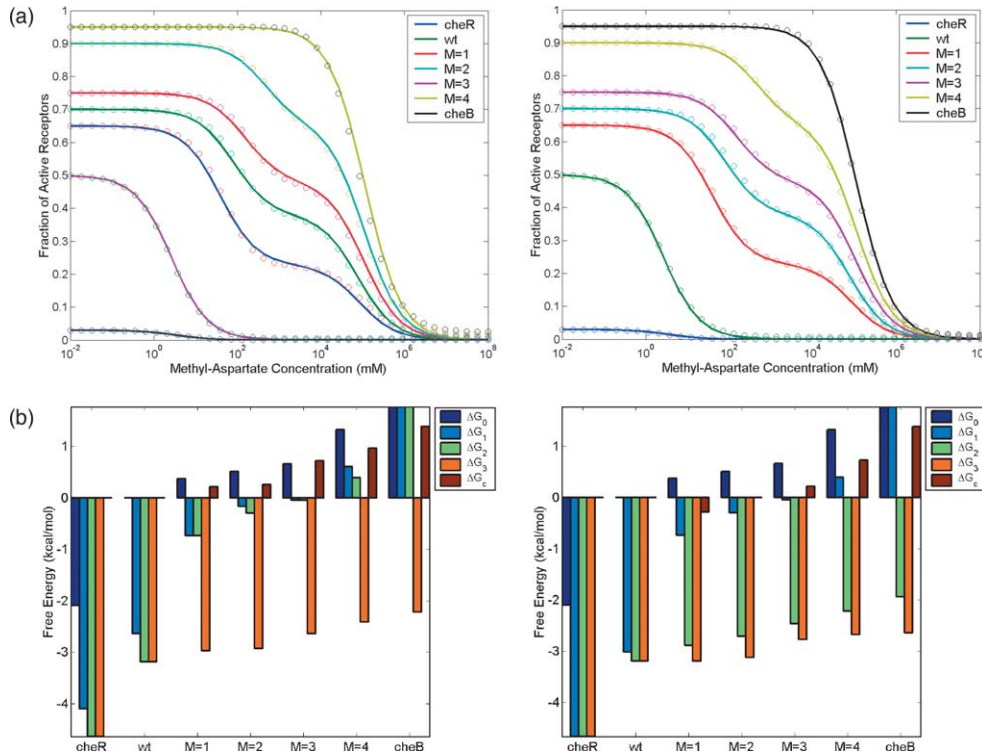


**Figure 6.** (a) The TD model applied to aspartate and serine receptors data. The left Figure denotes the results for TD receptor complexes with two Tar receptors and one Tsr receptor and the right Figure denotes the results for TD receptor complexes with one Tar receptor and two Tsr receptors. The circle markers denote the model and the continuous lines denote the data for the aspartate and serine receptors reported by Sourjik & Berg. Their data are presented as the solution of the equation:  $\beta(A_0K_1/(K_1 + L)) + (1 - \beta)(A_0K_2/(K_2 + L))$ , where for wild-type,  $A_0=0.5$ ,  $K_1=2.6 \mu\text{M}$ ,  $K_2=2.6 \mu\text{M}$ , and  $\beta=1$ ; for *cheR*,  $A_0=0.03$ ,  $K_1=3.3 \mu\text{M}$ ,  $K_2=3.3 \mu\text{M}$ , and  $\beta=1$ ; for  $m=0$ ,  $A_0=0.65$ ,  $K_1=38 \mu\text{M}$ ,  $K_2=83 \text{ mM}$ , and  $\beta=0.65$ ; for  $m=1$ ,  $A_0=0.75$ ,  $K_1=80 \mu\text{M}$ ,  $K_2=77 \text{ mM}$ , and  $\beta=0.46$ ; for  $m=2$ ,  $A_0=0.8$ ,  $K_1=150 \mu\text{M}$ ,  $K_2=105 \text{ mM}$ , and  $\beta=0.36$ ; for  $m=3$ ,  $A_0=0.9$ ,  $K_1=440 \mu\text{M}$ ,  $K_2=110 \mu\text{M}$ , and  $\beta=0.27$ ; and for *cheB*,  $A_0=0.95$ ,  $K_1=75 \text{ mM}$ ,  $K_2=75 \text{ mM}$ , and  $\beta=0$ . (b) Parameters for the TD model. The left Figure denotes the results for the TD receptor complexes with two Tar receptors and one Tsr receptor and the right Figure denotes the results for TD receptor complexes with one Tar receptor and two Tsr receptors. For all methylation states, the affinity for ligand is  $K(A_{00} \rightleftharpoons A_{10}) = 200 \mu\text{M}$  and  $K(A_{00} \rightleftharpoons A_{01}) = 10 \text{ M}$ .

single  $K_m$ , though the difference may be due to the sensitivity of their assay (Dunten & Koshland recorded the behavior of swimming cells, whereas Sourjik & Berg measured changes in phosphorylated CheY) or differences between D-aspartate and methyl-aspartate. Despite the differences, both studies clearly demonstrate that different kinds of receptors interact with one another by altering the stability of the signaling complex.

The trend in the estimated parameters for the mixed TD model is the same as the homo-TD model (Figures 4(b) and 6(b)). The difference is that with the mixed-TD model the subunits do not have the same affinity for ligand. This difference means that the sensitivity to ligand for the transition characterized by  $\Delta G_1$  is far greater than the sensitivity to ligand for the transition characterized by  $\Delta G_3$ . If the free energy change is large for either ( $\Delta G_0 - \Delta G_1$ ) or ( $\Delta G_1 - \Delta G_2$ ), then the receptor complex is destabilized at very low concentrations of ligand. If, on the other hand, the free energy changes for ( $\Delta G_0 - \Delta G_1$ ) and ( $\Delta G_1 - \Delta G_2$ ) are negligible, then the receptor complex is destabilized only at very high concentrations of ligand. When the changes in free energy for both ( $\Delta G_0 - \Delta G_1$ ) and ( $\Delta G_1 - \Delta G_2$ ) are neither large nor small, then there are two apparent  $K_m$  values. In terms of the Sourjik & Berg data, the relative values of the free energy  $\Delta G_1$  and, to a lesser extent,  $\Delta G_c$  are the dominant parameters (Figure

6(b)). These parameters are characterized both by the modification state of the aspartate and the serine receptors. In this regard, the model parameters are characterized by the collective behavior of the subunits within the complex.

These results still do not explain how bacteria are able to sense gradients equally well over such a wide range of concentrations. To explore the mixed-TD model further, we plotted the fraction of active complexes as a function of ligand at different values of the four parameters  $\Delta G_0$ ,  $\Delta G_1$ ,  $\Delta G_3$ , and  $\Delta G_c$  for a configuration with two Tar receptors and one Tsr receptor (Figure 7). Of the four parameters, it is clear that  $\Delta G_1$  has the greatest effect on the sensitivity, as the other two parameters control sensitivity only at higher concentrations of ligand. Based on these results, we hypothesized that  $\Delta G_1$  is the dominant parameter controlling sensitivity. In other words, the model predicts that the most sensitive parameter is the stability of the active state when one subunit is bound with ligand.

To test this hypothesis, we generated a series of ligand-response curves for different values of  $\Delta G_1$ . At each concentration, we picked the value of  $\Delta G_1$  for which the sensitivity is the greatest: the value that causes the greatest change in activity for a 10% increase in ligand concentration. These results predict that cells are able to sense gradients over a range of concentrations spanning almost six orders

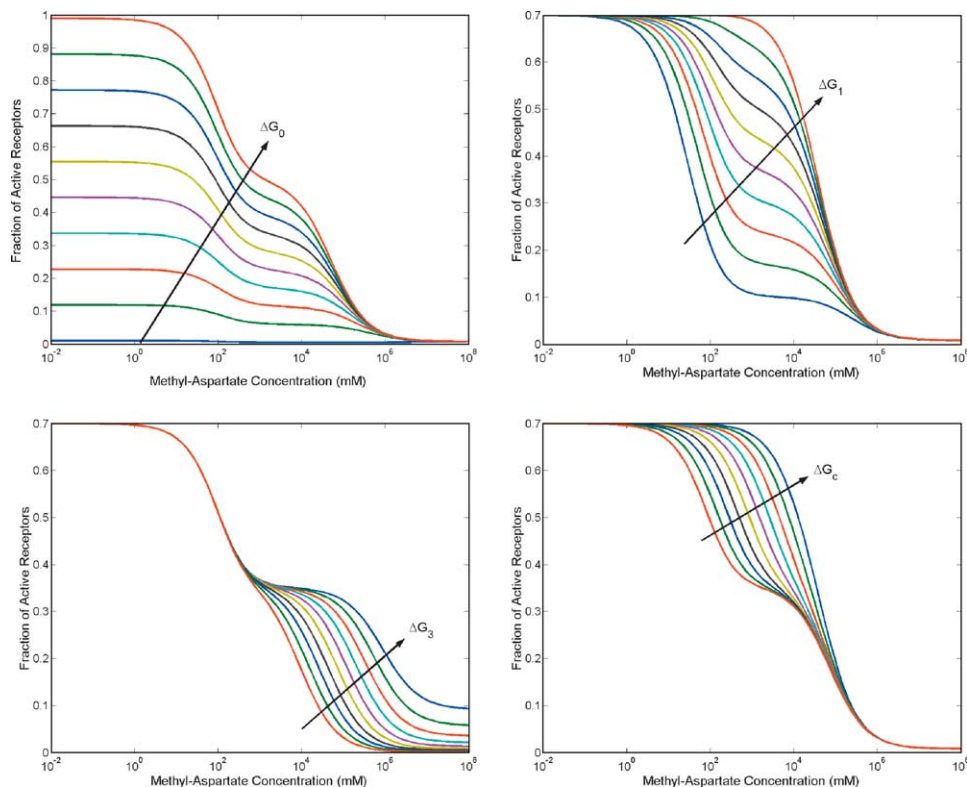


**Figure 7.** Parametric sensitivity of the mixed-TD model. The nominal model parameters are  $K(A_{00} \rightleftharpoons A_{10}) = 200 \mu\text{M}$ ,  $K(A_{00} \rightleftharpoons A_{01}) = 10 \text{ M}$ ,  $\Delta G_0 = 0.5 \text{ kcal/mol}$ ,  $\Delta G_1 = \max(-0.2 \text{ kcal/mol}, \Delta G_0)$ ,  $\Delta G_2 = \max(-0.4 \text{ kcal/mol}, \Delta G_1)$ ,  $\Delta G_3 = -2.9 \text{ kcal/mol}$ , and  $\Delta G_c = -0.25 \text{ kcal/mol}$ . The remaining parameters were determined by the thermodynamic linkage conditions. The ligand-response curves were generated by varying one parameter with respect to the nominal parameters. The arrows indicate how the model changes when a specific parameter is increased.

of magnitude by just increasing  $\Delta G_1$  (Figure 8). The model also predicts that the sensitivity has two maxima at concentrations of 25  $\mu\text{M}$  and 25 mM, respectively. By examining the free energy  $\Delta G_1$  for which the sensitivity is maximal, it is evident that the first peak is associated when a single kind of receptor (Tar) can destabilize a mixed complex and the second when both kinds of receptors (Tar and Tsr) are necessary to destabilize a mixed complex. Similar trends were reported in the experimental study by Sourjik & Berg,<sup>15</sup> though they report maximal sensitivity at concentrations of 100  $\mu\text{M}$  and 10 mM. The differences are expected, as we varied only a single parameter, and receptor methylation likely changes all four parameters. Based on these results, the model predicts that bacteria modulate their sensitivity by increasing the stability of the receptor complex, a process controlled by receptor methylation.

### Clustering

Sourjik & Berg,<sup>31</sup> in a second study, measured the

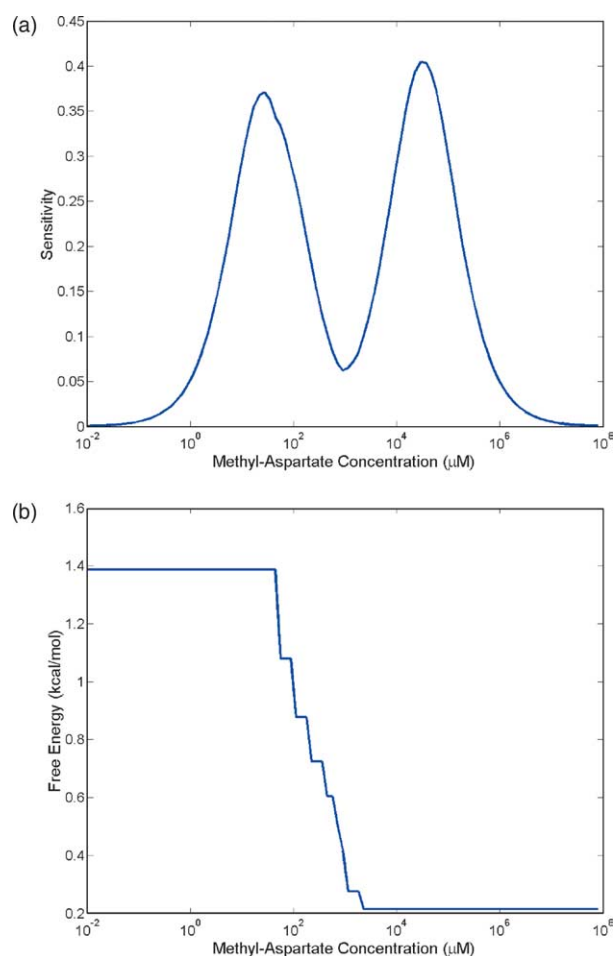


**Figure 8.** (a) Sensitivity to ligand for the mixed-TD model as a function of  $\Delta G_1$  for a 10% increase in aspartate concentration. Sensitivity is defined as:  $(A(L + \Delta L) - A(L))/\Delta L$ , where  $\Delta L = 0.1L$ . (b) Value of  $\Delta G_1$  when the sensitivity is maximized for a 10% increase relative to background concentration of aspartate.

effect of methyl-aspartate and serine on CheA activity *in vivo* by varying the expression of the aspartate and serine receptors, CheA, and CheW. Significant cooperativity was observed when either the concentration of receptors or CheW in the cell was increased. However, cooperativity decreased with increasing concentrations of CheA. Because the range of cooperativity is so broad (from 2 to 11 in the case of the aspartate receptor), their data suggest a range of clusters that depend on the concentrations of receptors, CheA, and CheW. To explore this hypothesis, we used a Monte-Carlo model where TD receptor complexes aggregate with CheA and CheW on a triangular lattice.

The results of the Monte-Carlo simulations are summarized in Figure 9, where the degree of clustering is the average number of TD receptor complexes bound to each CheA dimer. Expression of CheW modulates the degree of clustering biphasically, consistent with previous experimental measurements.<sup>2</sup> At relatively low concentrations of CheW, the degree of clustering is small because there is insufficient CheW to couple all of the TD receptor complexes to CheA. At relatively high concentrations, the degree of clustering is also small because CheW inhibits the formation of clusters by instead forming receptor-CheW and CheW-CheA intermediates. Maximal clustering is achieved when CheW is expressed at intermediate concentrations. Expression of the receptors increases the degree of clustering monotonically, as there are more TD receptor complexes to bind CheA. Expression of CheA, on the other hand, decreases the degree of clustering by effectively shifting the curves to the left (results not shown).

Collectively, these results explain many of the experimental observations made by Sourjik & Berg.<sup>31</sup> As the degree of clustering increases from 1 to 3, the maximum cooperativity for the associated allosteric model increases from 3 to 9 (results not shown). These numbers approach the measurements made by Sourjik & Berg (11 for the aspartate receptor and 10 for the serine receptor when over-expressed). They also explain the different cooperativity measurements made for the same kind of receptor by different groups. As noted by Bornhorst & Falke,<sup>16</sup> the receptor densities in some of these *in vitro* assays are greater than wild-type levels. Perhaps, the measurements made by Li & Weis<sup>41</sup> and Levit & Stock<sup>38</sup> are different because of expression. By increasing the number of receptors, the degree of clustering between adjacent TD receptor complexes increases and, as a result, the cooperativity also increases. Such a hypothesis is consistent with the model and measurements made by Sourjik & Berg.<sup>31</sup>

### Discussion

Using an allosteric model based on the TD model, we were able to integrate a diverse set of data using known signaling mechanisms. The overall

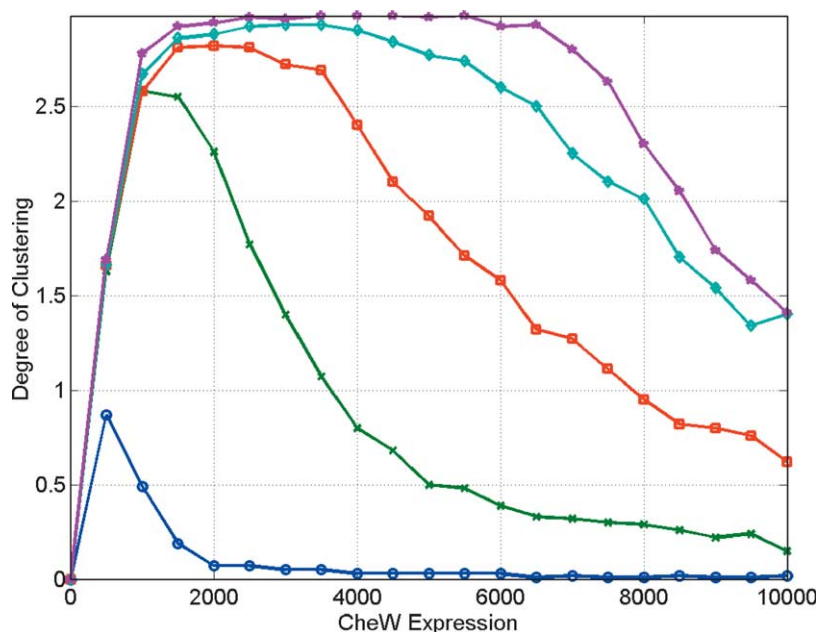


**Figure 9.** Clustering and the role of protein expression. Simulations were performed on a  $100 \times 100$  triangular lattice with periodic boundary conditions, the parameters  $\Delta G_{RW} = \Delta G_{AW} = -0.8$  kcal/mol, and 250 CheA molecules. Two million Monte-Carlo steps were used to generate each data point. The number of receptors were 100 (circles), 600 ( $\times$ -marks), 1100 (squares), 1700 (diamonds), and 2100 (stars).

conclusion is that the TD model is consistent with both the *in vitro* and *in vivo* experiments if we allow the TD receptor complexes to aggregate into larger cooperative structures. The conclusions are appealing as the experimental data are arguably converging towards this molecular model. In fact, we are not the first to propose this molecular model<sup>23–25</sup> and sought instead to show that an allosteric mechanism based on this model is in fact consistent with the data.

Enteric bacteria are the paradigm for chemotaxis, though the paradigm does not translate to all species of bacteria. Despite the differences, all known motile species of bacteria have homologues to the *E. coli* transmembrane receptors, CheW, and CheA.<sup>42</sup> The question then is whether the same signaling mechanism is conserved in divergent species of bacteria. In the case of *Bacillus subtilis*, different kinds of receptors can compensate for methylation defects in the asparagine (McpB) receptor.<sup>43</sup> These results suggest that mixed receptors may interact with one another in *B. subtilis* using a mechanism similar to *E. coli*. Whether the receptors form trimers of dimers or utilize alternate mechanisms to increase sensitivity is still unknown.<sup>44</sup>

Two aspects that we did not address with the model are adaptation and localization. It has previously been suggested that CheB phosphorylation plays an integral role in sensitivity.<sup>7</sup> We are currently attempting to integrate the proposed allosteric mechanism into a model for the full chemotaxis pathway. The challenge is that we need to integrate parameter estimates from multiple, often heterogeneous, sources of data. Finally, the model provides minimal insight regarding clustering and polar localization. Obviously, the lattice model is consistent with localization, but it does not explain why the receptors localize to the

cell poles, as the model often, depending on the parameters, predicts numerous small clusters uniformly distributed on the surface of the cell. One hypothesis orthogonal to the formation of cooperative structures is that localization increases the concentration of kinase and, as a result, the rate of messenger (CheY) phosphorylation.<sup>45</sup> It also could be that localization has nothing to do with sensitivity and, perhaps, is involved in methylation and adaptation.<sup>24,46</sup>

## Acknowledgements

This work was generously supported by HHMI, DOE, and DARPA. We thank the anonymous referees for their constructive criticism and suggestions.

## References

1. Bren, A. & Eisenbach, M. (2000). How signals are heard during bacterial chemotaxis: protein-protein interactions in sensory signal propagation. *J. Bacteriol.* **182**, 6865–6873.
2. Gegner, J. A., Graham, D. R., Roth, A. F. & Dahlquist, F. W. (1992). Assembly of an MCP receptor, CheW, and kinase CheA complex in the bacterial chemotaxis signal transduction pathway. *Cell*, **70**, 975–982.
3. Borkovich, K. A., Kaplan, N., Hess, J. F. & Simon, M. I. (1989). Transmembrane signal transduction in bacterial chemotaxis involves ligand-dependent activation of phosphate group transfer. *Proc. Natl Acad. Sci. USA*, **86**, 1208–1212.
4. Cluzel, P., Surette, M. & Leibler, S. (2000). An ultrasensitive bacterial motor revealed by monitoring signaling proteins in single cells. *Science*, **287**, 1652–1655.

5. Borkovich, K. A., Alex, L. A. & Simon, M. I. (1992). Attenuation of sensory receptor signaling by covalent modification. *Proc. Natl Acad. Sci. USA*, **89**, 6756–6760.
6. Goy, M. F., Springer, M. S. & Adler, J. (1977). Sensory transduction in *Escherichia coli*: role of a protein methylation reaction in sensory adaptation. *Proc. Natl Acad. Sci. USA*, **74**, 4964–4968.
7. Barkai, N., Alon, U. & Leibler, S. (2001). Robust amplification in adaptive signal transduction networks. *C. R. Acad. Sci. Paris, ser. IV*, **2**, 817–877.
8. Barkai, N. & Leibler, S. (1997). Robustness in simple biochemical networks. *Nature*, **387**, 913–917.
9. Hauri, D. C. & Ross, J. (1995). A model of excitation and adaptation in bacterial chemotaxis. *Biophys. J.* **68**, 708–722.
10. Morton-Firth, C. J., Shimizu, T. S. & Bray, D. (1999). A free-energy-based stochastic simulation of the Tar receptor complex. *J. Mol. Biol.* **286**, 1059–1074.
11. Shimizu, T. S., Aksenov, S. V. & Bray, D. (2003). A spatially extended stochastic model of the bacterial chemotaxis signalling pathway. *J. Mol. Biol.* **329**, 291–309.
12. Spiro, P. A., Parkinson, J. S. & Othmer, H. G. (1997). A model of excitation and adaptation in bacterial chemotaxis. *Proc. Natl Acad. Sci. USA*, **94**, 7263–7268.
13. Mesibov, R., Ordal, G. W. & Adler, J. (1973). The range of attractant concentrations for bacterial chemotaxis and the threshold and size of response over this range. Weber law and related phenomena. *J. Gen. Physiol.* **62**, 203–223.
14. Segall, J. E., Block, S. M. & Berg, H. C. (1986). Temporal comparisons in bacterial chemotaxis. *Proc. Natl Acad. Sci. USA*, **83**, 8987–8991.
15. Sourjik, V. & Berg, H. C. (2002). Receptor sensitivity in bacterial chemotaxis. *Proc. Natl Acad. Sci. USA*, **99**, 123–127.
16. Bornhorst, J. A. & Falke, J. J. (2000). Attractant regulation of the aspartate receptor-kinase complex: limited cooperative interactions between receptors and effects of the receptor modification state. *Biochemistry*, **39**, 9486–9493.
17. Alley, M. R., Maddock, J. R. & Shapiro, L. (1992). Polar localization of a bacterial chemoreceptor. *Genes Dev.* **6**, 825–836.
18. Maddock, J. R. & Shapiro, L. (1993). Polar location of the chemoreceptor complex in the *Escherichia coli* cell. *Science*, **259**, 1717–1723.
19. Sourjik, V. & Berg, H. C. (2000). Localization of components of the chemotaxis machinery of *Escherichia coli* using fluorescent protein fusions. *Mol. Microbiol.* **37**, 740–751.
20. Bray, D., Levin, M. D. & Morton-Firth, C. J. (1998). Receptor clustering as a cellular mechanism to control sensitivity. *Nature*, **393**, 85–88.
21. Duke, T. A. & Bray, D. (1999). Heightened sensitivity of a lattice of membrane receptors. *Proc. Natl Acad. Sci. USA*, **96**, 10104–10108.
22. Kim, S. H., Wang, W. & Kim, K. K. (2002). Dynamic and clustering model of bacterial chemotaxis receptors: structural basis for signaling and high sensitivity. *Proc. Natl Acad. Sci. USA*, **99**, 11611–11615.
23. Shimizu, T. S., Le Novere, N., Levin, M. D., Beavil, A. J., Sutton, B. J. & Bray, D. (2000). Molecular model of a lattice of signalling proteins involved in bacterial chemotaxis. *Nature Cell Biol.* **2**, 792–796.
24. Falke, J. J. (2002). Cooperativity between bacterial chemotaxis receptors. *Proc. Natl Acad. Sci. USA*, **99**, 6530–6532.
25. Kim, K. K., Yokota, H. & Kim, S. H. (1999). Four-helical-bundle structure of the cytoplasmic domain of a serine chemotaxis receptor. *Nature*, **400**, 787–792.
26. Ames, P., Studdert, C. A., Reiser, R. H. & Parkinson, J. S. (2002). Collaborative signaling by mixed chemoreceptor teams in *Escherichia coli*. *Proc. Natl Acad. Sci. USA*, **99**, 7060–7065.
27. Studdert, C. A. & Parkinson, J. S. (2004). Crosslinking snapshots of bacterial chemoreceptor squads. *Proc. Natl Acad. Sci. USA*, **101**, 2117–2122.
28. Dunten, P. & Koshland, D. E., Jr (1991). Tuning the responsiveness of a sensory receptor via covalent modification. *J. Biol. Chem.* **266**, 1491–1496.
29. Mello, B. A. & Tu, Y. (2003). Quantitative modeling of sensitivity in bacterial chemotaxis: the role of coupling among different chemoreceptor species. *Proc. Natl Acad. Sci. USA*, **100**, 8223–8228.
30. Gestwicki, J. E. & Kiessling, L. L. (2002). Inter-receptor communication through arrays of bacterial chemoreceptors. *Nature*, **415**, 81–84.
31. Sourjik, V. & Berg, H. C. (2004). Functional interactions between receptors in bacterial chemotaxis. *Nature*, **428**, 437–441.
32. Albert, R., Chiu, Y. & Othmer, H. G. (2004). Dynamic receptor team formation can explain the high signal transduction gain in *E. coli*. *Biophys. J.* **86**, 2650–2659.
33. Zhang, C. & Kim, S. H. (2000). The effect of dynamic receptor clustering on the sensitivity of biochemical signaling. *Pac. Symp. Biocomput.* 353–364.
34. Monod, J., Wyman, J. & Changeux, J. P. (1965). On the nature of allosteric transitions: a plausible model. *J. Mol. Biol.* **12**, 88–118.
35. Falke, J. J. & Hazelbauer, G. L. (2001). Transmembrane signaling in bacterial chemoreceptors. *Trends Biochem. Sci.* **26**, 257–265.
36. Homma, M., Shiomi, D. & Kawagishi, I. (2004). Attractant binding alters arrangement of chemoreceptor dimers within its cluster at a cell pole. *Proc. Natl Acad. Sci. USA*, **101**, 3462–3467.
37. Bornhorst, J. A. & Falke, J. J. (2001). Evidence that both ligand binding and covalent adaptation drive a two-state equilibrium in the aspartate receptor signaling complex. *J. Gen. Physiol.* **118**, 693–710.
38. Levit, M. N. & Stock, J. B. (2002). Receptor methylation controls the magnitude of stimulus-response coupling in bacterial chemotaxis. *J. Biol. Chem.* **277**, 36760–36765.
39. Biemann, H. P. & Koshland, D. E., Jr (1994). Aspartate receptors of *Escherichia coli* and *Salmonella typhimurium* bind ligand with negative and half-of-the-sites cooperativity. *Biochemistry*, **33**, 629–634.
40. Goldman, J., Andrews, S. & Bray, D. (2004). Size and composition of membrane protein clusters predicted by Monte Carlo analysis. *Eur. Biophys. J.* In the press.
41. Li, G. & Weis, R. M. (2000). Covalent modification regulates ligand binding to receptor complexes in the chemosensory system of *Escherichia coli*. *Cell*, **100**, 357–365.
42. Armitage, J. P. (1999). Bacterial Tactic Response. In *Advances in Microbial Physiology*, vol. 41, pp. 229–289, Academic Press, London.
43. Zimmer, M. A., Szurmant, H., Saulmon, M. M., Collins, M. A., Bant, J. S. & Ordal, G. W. (2002). The role of heterologous receptors in McpB-mediated signalling in *Bacillus subtilis* chemotaxis. *Mol. Microbiol.* **45**, 555–568.
44. Rao, C. V., Kirby, J. R. & Arkin, A. P. (2004). Design

- and diversity in bacterial chemotaxis: a comparative study in *Escherichia coli* and *Bacillus subtilis*. *PLoS Biol.* **2**, E49.
45. Kholodenko, B. N. (2003). Four-dimensional organization of protein kinase signaling cascades: the roles of diffusion, endocytosis and molecular motors. *J. Expt. Biol.* **206**, 2073–2082.
46. Levin, M. D., Shimizu, T. S. & Bray, D. (2002). Binding and diffusion of CheR molecules within a cluster of membrane receptors. *Biophys. J.* **82**, 1809–1817.
47. Bray, D. (2002). Bacterial chemotaxis and the question of gain. *Proc. Natl Acad. Sci. USA*, **99**, 7–9.

*Edited by I. B. Holland*

(Received 16 March 2004; received in revised form 9 August 2004; accepted 11 August 2004)